Quantitative Comparison of Direct Antibody Labeling and Tumor Pretargeting in Uveal Melanoma

Patrizia Magnani, Giovanni Paganelli, Giulio Modorati, Felicia Zito, Cristina Songini, Francesco Sudati, Peter Koch, Helmut R. Maecke, Rosario Brancato, Antonio G. Siccardi and Ferruccio Fazio

INB-CNR, Departments of Ophthalmology and Nuclear Medicine, University of Milan, Institute H S. Raffaele, Milan, Italy; and Department of Nuclear Medicine, University of Basel, Basel, Switzerland

SPECT radioimmunoscintigraphy with ^{99m}Tc-labeled anti-melanoma monoclonal antibodies (MAbs) 225.28S is being used to detect uveal melanoma. Recently, pretargeting methods have been described to reduce background activity and perform imaging in a shorter time interval. **Methods:** We compared the three-step pretargeting method with conventional radioimmunoscintigraphy in 15 patients with a clinical and laboratory diagnosis of uveal lesion. High-resolution SPECT radioimmunoscintigraphy was performed in all patients with directly labeled MAbs and, 1 wk later, with the three-step pretargeting technique. Eleven patients underwent eye enucleation and specimens of uveal melanoma were available for histology, whereas four patients underwent conservative therapy. The percent injected dose (%ID) delivered to the tumor and the tumor-to-background ratio were calculated. **Results:** In all three-step radioimmunoscintigraphy studies, there was a reduction of nonspecific nasopharyngeal background. The three-step radioimmunoscintigraphy tumor-to-nontumor ratio was 3.1 ± 1.3 versus 1.5 ± 0.5 of conventional radioimmunoscintigraphy, while the percent injected dose on the tumor was similar for the two methods (4.4 ± 3.0 versus 3.8 ± 2.8) × 10^{-3}. **Conclusion:** Improved SPECT imaging with the three-step radioimmunoscintigraphy results from reduced background and from higher counting statistics due to reduction of time interval between radiotracer administration and imaging, whereas the absolute amount of tracer delivered to the tumor by the two methods is comparable.

Key Words: monoclonal antibodies; uveal melanoma; avidin/biotin; SPECT

J Nucl Med 1996; 37:967–971

Radioimmunoscintigraphy with monoclonal antibodies (MAbs) against melanoma associated antigens is a relatively new technique that can be used as an additional test to detect ocular melanomas in clinically difficult cases (*1–7*). However, some problems still limit the diagnostic (and therapeutic) potential of radioimmunoscintigraphy: the main problem is due to the unfavorable tumor-to-nontumor ratio (T/nT), related to the high level of circulating antibodies and their pharmacokinetics (*8*). In particular, nonspecific uptake in the bone marrow and mucous membranes of the nasopharynx makes interpretation of small lesions in the nasal quadrant of the eye difficult (*6*). In such cases, SPECT is useful because it helps to separate the activity in the tumor from the activity in the nasopharyngeal region and to define the lesion more clearly. Limiting factors for SPECT are the poor count rate in the field of view during imaging 6–8 hr postinjection (*5*) and the relatively poor spatial resolution of single-head rotating gamma cameras. Spatial resolution and detection efficiency of tomographic imaging are improved with high-resolution SPECT systems (*9*), which result in better image quality and improved quantification of regional radioactivity. The improvement in image quality obtained by high-resolution SPECT, however, does not diminish the limitations related to the kinetics of tracers used in radioimmunoscintigraphy. Among the various strategies proposed to overcome the problem of background activity, a method that uses tumor pretargeting with MAb and the avidin/biotin system has given encouraging results in the diagnosis of CEA-secreting solid carcinomas and offers several advantages over the administration of directly labeled MAbs. This strategy involves the injection of biotinylated MAbs (first step), followed by avidin administration (second step) to precipitate circulating biotinylated MAbs and, at the same time, to target the tumor cells for adequate homing in of the subsequently radiolabeled biotin (third step) (*10*).

The aim of this study was to compare quantitatively (tumor-to-nontumor ratio and percent injected dose delivered to the tumor), three-step and conventional radioimmunoscintigraphy in the same patients with uveal melanoma.

MATERIALS AND METHODS

Patients

Fifteen patients (Table 1) with a clinical diagnosis of choroidal melanoma were enrolled in the study approved by the Scientific Institute H San Raffaele Ethics Committee. Before study entry, all patients gave written informed consent. All tumors were clinically diagnosed by ophthalmoscopy, ultrasonography, fluorescein angiography and CT.

Inclusion criteria were: (a) volumes between 0.1 and 2.7 ml as assessed by CT scans, (b) no previous treatment of the lesion, (c) normal controlateral eye and (d) no metastases.

Specimens of uveal melanoma were obtained from 11 patients who underwent eye enucleation. The histopathological diagnosis was assessed on paraffin sections. Cell type was recorded as spindle cell, epitheloid cell or mixed cell type.

Immunohistochemistry was performed as previously described (*4*).

Four patients underwent conservative radiation therapy and no histopathology was performed.

Reagents and Radiolabeling

Directly Labeled MAbs. MAb 225.28S (IgG_{2a}) specific for the HMW-MAA antigen has been described and extensively utilized in immunoscintigraphy (*2–4*). IgG immunoglobulins were converted into $F(ab')_2$ fragments by pepsin digestion followed by purification by gel filtration to assure complete removal of any residues having Fc reactivity.

Radiolabeling of $F(ab')_2$ fragments was performed as previously described (*11*).

Pretargeting. MAb 225.28S whole IgG was supplied by Sorin Biomedica. Pure hen egg avidin was purchased from S.P.A. (Società Prodotti Antibiotici—S.P.A., Milan, Italy). The synthesis

Received Jun. 1, 1995; revision accepted Aug. 18, 1995.

For correspondence or reprints contact: Ferruccio Fazio, MD, Department of Nuclear Medicine, University of Milan, Scientific Institute H S. Raffaele, Via Olgettina 60, 20132 Milan, Italy.

TABLE 1
Patient Data

Patient no.	Lesion volume (ml)	Histology	IHC	T $F(ab')_2$	T Three-step
1	1.26	Mixed	+	6.8	2.0
2	1.37	Mixed	+	6.0	1.5
3	0.16	Spindle	+	8.0	2.3
4	0.90	Spindle	+	7.0	2.6
5	0.96	Spindle	+	6.3	2.5
6	0.11	n.a.	n.a.	6.0	2.0
7	1.05	Spindle	+	6.3	3.6
8	0.18	Spindle	−	6.0	2.0
9	0.27	Mixed	+	5.5	2.5
10	0.44	n.a.	n.a.	6.5	2.0
11	0.21	Mixed	n.a.	7.0	2.0
12	0.78	n.a.	n.a.	6.0	2.0
13	1.10	Mixed	+	6.0	1.5
14	0.26	n.a.	n.a.	6.0	2.0
15	2.70	Mixed	−	6.0	2.5
Mean ± s.d.				6.4 ± 0.6	2.2 ± 0.6

IHC = immunohistochemistry; T = time (hours) elapsing between injection of radioactivity and imaging; n.a. = not available.

of the biotin-dioxime derivate (PnAO-biotin) has been published elsewhere (*12*).

Biotinylation of the antibody has also been described (*13*). Briefly, biotinyl-aminocaproic acid N-hydroxysuccinimide ester in anhydrous dimethyl sulfoxide (1 mg/ml) was added to a solution of MAb 225.28S (1 mg/ml in 0.1 *M* sodium bicarbonate buffer, pH 8.5) at a ratio of 0.04:1. The mixture was gently stirred at room temperature for 4 hr and finally dialyzed overnight against PBS (pH 7.4). Biotinylation was verified by ELISA; the solid-phase was coated with rabbit anti-mouse antibodies and the biotinylated Ab was detected by an acetyl-avidin-biotinylated peroxidase complex. The degree of biotinylation was 5 ± 1 per antibody determined, after protein digestion, spectrophotometrically as described (*14*).

Immunoreactivity of biotinylated MAbs was tested in a standard ELISA system (solid-phase Colo 38 cells as catcher, peroxidase-coupled rabbit anti-mouse antibodies as tracer and unbiotinylated 225.28S MAb as control) as previously described (*13*). No loss of Ab immunoreactivity after biotinylation was detected.

Radiolabeling of PnAO-Biotin (12). Approximately 900 μg (1.49 μmole) PnAO-biotin were dissolved in 1 ml of EtOH/H_2O (1:1). To this solution, 500 μl KNa-tartrate-4 H_2O (161 mg/10 ml), 5 μl $SnCl_2$ − 2 H_2O (9 mg/10 ml) and 250 μl $^{99m}TcO_4^-$ generator saline eluate (about 40 mCi) were added and incubated at room temperature for 15 min at pH 8. After this time, complex formation was >99%.

Removal of unlabeled PnAO-biotin was done using a Sepak C18 cartridge. The above mixture was loaded onto the cartridge and free conjugate washed away with water. The labeled conjugate was eluted from the cartridge with methanol, which is easily evaporated. The residue was dissolved in 2 ml PBS-buffer.

Quality control was done by HPLC (C18, 5 μm, Bondapak, Waters) with an isocratic mobile phase of 40% 0.01 *M* ammonium acetate and 60% acetonitrile. The labeled conjugate elutes after 2.18 min. The binding capability to avidin was checked using avidin immobilized on beaded agarose or by mixing avidin (4 mg) with the labeled conjugate in PBS (pH 8.9) and subjecting the complex to gel filtration. Both controls gave essentially the same results. Binding was 98.1% ± 1.7% (6 runs).

High-Resolution SPECT Imaging Protocols

Conventional Radioimmunoscintigraphy. Fifteen to 20 mCi ^{99m}Tc-MAb were administered intravenously to each patient.

High-resolution SPECT imaging was performed 6–8 hr postinjection, as suggested in the literature (*1,5,11*), using an annular SPECT system with spatial resolution equal to 8.4 mm FWHM in the center of the axial plane. The system covered an axial field of view of 10.5 cm. The patient's head was positioned in a headholder specifically built for the annular SPECT camera. Setting the energy window at 140 keV ± 10%, 120 projections rotating over 360° were collected for 30 min with a matrix 128 × 64 (pixel size 1.64 mm).

Three-Step Radioimmunoscintigraphy. One week after the conventional radioimmunoscintigraphy study, the three-step protocol was used. This protocol has been described elsewhere (*10*). Briefly, 1 mg biotinylated MAb 225.28S was injected intravenously (first step). After 24 hr, 1 mg unlabeled avidin was injected intravenously, followed by an additional 5 mg 30 min later (second step). The aim of these two avidin administrations is to precipitate circulating biotinylated antibodies (1 mg) and subsequently (5 mg) to target the tumor cells which allows adequate homing in of the administered labeled biotin (third step). Two hundred μg [^{99m}Tc]P-nAO-biotin (15–20 mCi) were injected intravenously 24 hr after cold avidin administration.

High-resolution SPECT scans were obtained 1.5–2 hr postinjection, as in the conventional radioimmunoscintigraphy procedure described above.

Data Analysis

Sixty-four axial slices, 1.64 mm thick, were reconstructed with a Hann two-dimensional prefilter (cutoff 0.5 $pixel^{-1}$) and using a backprojection algorithm with a ramp filter. Attenuation correction was performed using Chang's method (*15*) with a coefficient of 0.1 cm^{-1}.

In all patients, SPECT quantitative parameters were assessed using the most representative transaxial slice crossing the center of the lesion and containing its maximum pixel value.

A small circular region of interest (ROI) (3 pixels in diameter) on the tumor, an irregular ROI on the nasopharynx (8 pixels in diameter) and a circular ROI (8 pixels in diameter) in the healthy contralateral orbit (BKG) were drawn and the count mean values were determined to assess the tumor-to-nontumor ratio and lesion radioactivity concentration. SPECT ROI localization was carefully established guided by CT scanning. The p value for the difference between the tumor and the BKG was also assessed by a one-tail, two-sample t-test (*16*). When the difference was significant ($p < 0.05$, for a t value greater than 1.3), lesion radioactivity concentration was determined taking into account system partial volume effects and the spillover due to the surrounding background. As background, the mean value BKG was considered.

System partial volume effects were studied on the basis of an experimental model consisting of six radioactive spheres with different volumes ranging from 0.4 to 26 ml mounted inside a uniform cylindrical phantom (5 cm off axis) filled with a nonradioactive solution. The hot sphere recovery coefficients were calculated as the ratio between measured/true concentration versus sphere volumes. According to these experimental data, the correspondent hot sphere radioactivity coefficient was calculated for each lesion of the known volume determined from the CT scan.

Counts per second per voxel on reconstructed slices were transformed into microcuries per milliliter (μCi/ml) using a calibration factor K. This factor was derived from a uniform cylindrical phantom (diameter = 20 cm) filled with a radioactive solution of ^{99m}Tc and using the same patient protocol for data acquisition and reconstruction. The radioactive concentration of the solution

(μCi/ml) was measured with a calibrated well counter using withdrawn samples of 1 ml.

Lesion concentration corrected for background and partial volume (A*) was determined according to the Kessler formula (*17*) as:

$$A^* = [(T - BKG)/HSRC + BKG]/K.$$

The tumor percent of activity (%id) at the time of imaging was assessed as:

$$100 \times (A^* \times V)/id,$$

where id was the injected dose.

Finally the tumor percent activity was corrected for the physical decay of ^{99m}Tc between injection and imaging to calculate the actual percent injected dose (%ID) targeted onto the tumor.

Toxicity and Immunogenicity Assessment

All patients were closely observed for 2 hr after administration of avidin. Blood samples (10 ml) were obtained in appropriate tubes just before the avidin administration, then 2 days and, when possible, 2 wk following the injection. All samples were sent out for routine blood tests as well as to assess the human anti-mouse immunoglobulin and anti-avidin response.

The induction of human anti-mouse immunoglobulin antibodies (HAMA) was verified using an ELISA system (*18*) in nine patients. Avidin immunogenicity (HAAR) was studied in nine patients on microwell plates coated with avidin or streptavidin separately. The plates were saturated for 1 hr with PBS-3% BSA. Human sera dilutions were added and incubated for 1 hr at 37°C. After five washes, the binding of human anti-avidin antibodies was revealed with horseradish peroxidase-conjugated rabbit anti-human Ig antibodies (DAKO) diluted 1:1000 for 45 min at 37°C. After six washes, the enzymatic reaction was developed with a chromogenic substrate for 10 min and blocked by addition of 1 *M* H_2SO_4. The optical density reading was at 492 nm.

RESULTS

High-Resolution SPECT Imaging

Patient data and radioimmunoscintigraphy results are summarized in Tables 1 and 2.

In 11 patients (Patients 1, 2, 3, 4, 5, 6, 7, 9, 10, 13, 14) the t value was higher than 10, whereas in Patients 8, 11, 12 and 15, the t value was not significantly higher than the BKG value (incidentally, the tumor value was lower than BKG). In these last patients, %id and %ID were not calculated.

Three-step radioimmunoscintigraphy tumor-to-nontumor ratios ranged from 1.4 to 5.7 (mean = 3.1 ± 1.3) versus 0.7–2.4 (mean = 1.5 ± 0.5) of conventional radioimmunoscintigraphy (Patients 8, 11, 12 and 15 excluded). The difference in tumor-to-nontumor ratios using the two methods was highly significant using paired t test (*16*), when the above patients were included ($p < 0.0015$) as well were excluded ($p < 0.0006$).

The absence of lesion uptake in Patients 8 and 15 was due to a lack of antigenic expression of the HMW-MAA antigen by the tumor cells, as verified by immunohistochemistry, performed as previously described (*4*). Immunoreactivity of the tumor in Patients 6, 10, 11, 12 and 14 could not be assessed since MAb 225.28S reacts with frozen sections only (*4*), which were not available in Patient 11, whereas Patients 6, 10, 12 and 14 underwent conservative therapy and histology and immunohistochemistry were not performed. Immunohistochemistry showed expression of the HMW-MAA antigen in all the other melanomas.

The tumor percent of activity delivered to the tumor at the time of SPECT imaging was (mean = 3.5 ± 2.4) × 10^{-3} for the three-step method and (mean = 1.9 ± 1.2) × 10^{-3} for $F(ab')_2$. This difference was largely due to the different time interval required by the two-methods between injection of radioactivity and imaging. Indeed, by correcting the tumor percent of activity for the physical decay of ^{99m}Tc (%ID), no significant differences were observed between the two methods (mean = 4.4 ± 3.0 versus mean = 3.8 ± 2.8) × 10^{-3}.

TABLE 2
Radioimmunoscintigraphy Results

Patient no.	%id* $F(ab')_2$	%id* Three-step	%ID $F(ab')_2$	%ID* Three-step	T/nT $F(ab')_2$	T/nT Three-step
1	4.8	8.5	10.4	10.7	1.7	4.5
2	3.4	6.7	6.9	8.0	1.5	5.7
3	0.8	1.4	2.0	1.9	2.0	3.0
4	2.4	4.9	5.5	6.6	1.0	1.8
5	1.1	1.5	2.3	2.0	0.9	1.7
6	0.6	1.0	1.2	1.4	1.5	3.5
7	1.7	3.5	3.5	5.2	1.0	1.7
8	n.c.	n.c.	n.c.	n.c.	*0.3*	*0.4*
9	1.3	2.7	2.5	3.6	1.4	4.1
10	1.2	2.7	2.6	3.5	2.4	3.8
11	n.c.	n.c.	n.c.	n.c.	*0.3*	*0.3*
12	n.c.	n.c.	n.c.	n.c.	*0.3*	*0.2*
13	1.8	3.4	3.9	4.1	2.0	3.3
14	0.8	1.3	1.7	1.7	0.7	1.4
15	n.c.	n.c.	n.c.	n.c.	*0.1*	*0.1*
Mean ± s.d.	1.9 ± 1.2	3.5 ± 2.4	3.8 ± 2.8	4.4 ± 3.0	1.5 ± 0.5	3.1 ± 1.3

*× 10^{-3}.

%id = percent activity measured on tumor at the time of imaging; %ID = percent injected dose delivered to the tumor (decay-corrected); n.c. = not calculated because T was not significantly higher than BKG.

Note: Numbers in italics were not used in the calculation of mean and s.d.

Figure 1A is the conventional radioimmunoscintigraphy study of Patient 1 performed 6.8 hr after ^{99m}Tc-MAb injection. Relevant uptake is visible in the tumor lesion located in the left eye. Activity is also present in the nasopharyngeal area. Figure 1B is the three-step radioimmunoscintigraphy study performed 90 min postinjection of [^{99m}Tc]PnAO-biotin in the same patient. The tumor is clearly visualized and background noise within the orbit and in the surrounding areas was drastically reduced.

Figure 2 depicts the radioimmunoscintigraphy studies of Patient 3 who had a right eye melanoma. In this patient, conventional radioimmunoscintigraphy (Fig. 2A) failed to visualize the tumor, which was masked by the background

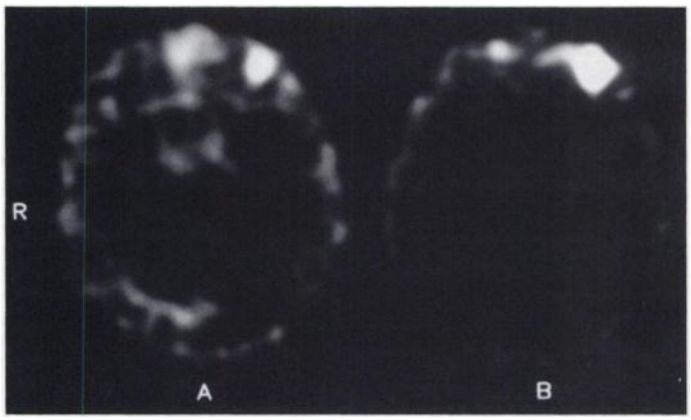

FIGURE 1. Conventional (A) and three-step radioimmunoscintigraphy (B) in Patient 1. Relevant uptake of radiotracer is visible in the left eye, with low background present at 2 hr postinjection (B).

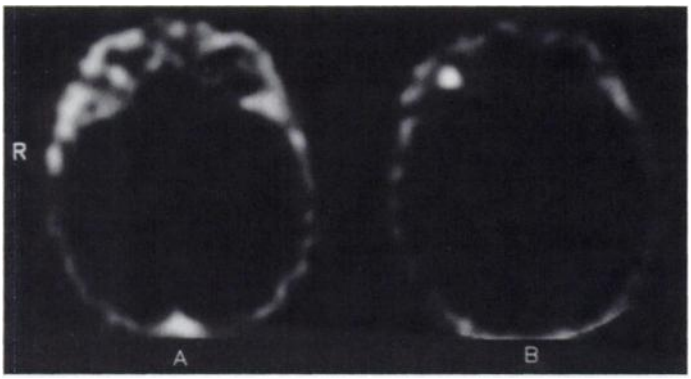

FIGURE 2. Conventional (A) and three-step radioimmunoscintigraphy (B) in Patient 3. Weak tracer uptake in the right eye in conventional radioimmunoscintigraphy can be identified as tumor uptake only on the basis of the morphological study and three-step radioimmunoscintigraphy. In this study, the lesion is clearly visible.

activity. On the other hand, three-step radioimmunoscintigraphy (Fig. 2B) showed significant radiotracer uptake in the right eye.

Toxicity and Immunogenicity

No acute toxicity nor alterations of liver or renal functions were observed after reagents injection. None of the nine patients studied developed an antibody response against mouse immunoglobulins nor anti-avidin antibodies 15–20 days postinjection.

DISCUSSION

Clinical Use of Radioimmunoscintigraphy in Ocular Melanoma

The use of radiolabeled MAbs, specific for the HMW-MAA antigen, which is expressed by nearly 90% of melanomas, has been reported for the diagnosis of ocular melanoma in clinically difficult cases (*1,5–7*). Indeed, there are several sources of uncertainty in the clinical diagnosis of tumor in the uvea. A small pigmented malignant melanoma can be difficult to distinguish from a benign nevus, a melanocytoma or a carcinoma of the retinal pigmented epithelium. On the other hand, it may not be easy to decide whether a nonpigmented mass lesion is an amelanotic melanoma, a choroidal hemangioma or a choroidal metastasis. The presence of opaque ocular media (corneal leucoma, cataract, vitreous hemorrhage, retinal detachment) represents an additional difficulty (*19–24*). Other uncertainties may arise when conservative therapy of uveal malignant melanoma is considered (*5,25*). Small melanomas can be destroyed in situ by photocoagulation or radiation with good visual results and in this case a tissue diagnosis may never be obtained. Although choroidal biopsy is technically possible, many melanomas are too posterior for the procedure to be contemplated without undue risk of complications. Therefore, the success of these conservative therapeutic techniques might increase if confirmation of the nature of the tumor could be obtained by using a tumor-specific imaging technique, such as radioimmunoscintigraphy.

The characteristics which define a good tumor marker for imaging are its sensitivity and specificity for the individual tumor. One of the factors which influences the sensitivity of the test is the ability to detect these small amounts of radioactivity. This is dependent on various factors, such as the resolution and the sensitivity of the imaging system used, the technique applied, the tumor volume, the percent injected dose on the tumor and the tumor-to-nontumor ratio. In patients with CEA-expressing carcinomas (*10*), and recently in glioma and lung cancer patients (*26,27*), pretargeted three-step radioimmunoscintigraphy showed a reduction of background radioactivity and consequently a higher tumor-to-nontumor ratio compared to conventional radioimmunoscintigraphy.

Direct Antibody Labeling Versus Pretargeting

In this study, the sensitivity of conventional and three-step radioimmunoscintigraphy performed in the same patient (same lesion) using a high-resolution SPECT camera was compared in terms of reduction of background radioactivity, tumor-to-nontumor ratio and in vivo tumor signal amplification (%ID on the tumor). At the moment of image acquisition, the three-step radioimmunoscintigraphy tumor-to-nontumor ratio was always greater than that of conventional radioimmunoscintigraphy.

This favorable three-step radioimmunoscintigraphy tumor-to-nontumor ratio, obtained only 2 hr postinjection, and the better counting statistics due to the reduction of the time interval between radiotracer administration and tomography resolves one of the limiting factors for SPECT, i.e., the poor count rate during imaging (*5*). Lesions detected by radioimmunoscintigraphy using the three-step method were smaller (Patients 3 and 6) and/or situated in the nasal quadrant of the eye (Patient 5). Their visualization was possible thanks to the increased ratio between tumor and background activity (mean = 3.1 ± 1.3 versus mean = 1.5 ± 0.5), which is due to nonspecific uptake of directly-labeled antibodies in the bone marrow and the mucous membranes of the nasopharynx.

This study indicates that the increased tumor-to-nontumor ratio of the three-step approach is mainly due to a reduction of the background which is obtained by removal with cold avidin (second step) of circulating antibodies. Indeed, the increased tumor percent activity obtained with the three-step method is due to the shorter time elapsing between injection of radioactivity and imaging rather than to antibody signal amplification due to free binding sites of the avidin molecule. This is shown by the lack of differences in the percent injected dose between the three-step and the conventional $F(ab')_2$ method when tumor percent activity data are normalized for radioactive decay of ^{99m}Tc (Table 2).

Generally, the favorable tumor-to-nontumor ratio and consequently the higher sensitivity of three-step radioimmunoscintigraphy in the detection of ocular melanoma can allow wider clinical application of the technique. Small lesions, situated in the nasal quadrant of the eye or in the presence of opaque ocular media, may be visualized and correctly diagnosed with a consequent better therapeutic approach.

The capability of the imaging technique in distinguishing between benign and malignant disease is strictly associated to the specificity of MAb 225.28S for the HMW-MAA antigen. All tumor markers presently used are not specific for a certain tumor; they are just expressed in a higher quantity by malignancies compared with normal tissue. Normal eyes do not react with antibodies against the HMW-MAA antigen. Some authors occasionally reported antibody accumulation in choroidal nevi (*28*), whereas intraocular metastases are negative. This makes radioimmunoscintigraphy with MAbs against HMW-MAA antigen a valuable diagnostic method which offers substantial sensitivity and specificity for the differentiation of intraocular lesions, particularly choroidal melanoma, nevus and metastasis (*29*).

The immunogenicity of biotinylated antibodies and avidin was tested in only nine patients. Data available from 66 other patients receiving, in similar protocols, biotinylated antibodies (i.e., anti-tenascin and anti-CEA) and avidin agree with the results of this study. In particular, 6% of the patients studied developed HAMA after the injection of 1–2 mg biotinylated

IgG and only the 21% developed HAAR after the injection of 5–6 mg avidin (*30*).

Future Perspectives

An additional potential advantage of this pretargeting technique is that the second and third step of the three-step protocol can be common to all studies, irrespective of the specificity of the anti-tumor MAb, and potentially useful MAb can be injected in sequence or even in combination as the first step. Thus, tumor pretargeting of uveal melanoma can be exploited at its best using cocktails of MAbs that recognize different tumor-associated antigens. This could avoid false-negative studies that may occur due to immunological heterogeneity of uveal melanoma and increase tumor activity as demonstrated in animal models (*31,32*).

With this method, radiolabeled biotin can serve as a carrier not only for diagnostic but also for therapeutic isotopes such as ^{90}Y and ^{188}Re. Indeed the longer plasma T½ and the higher tissues retention of streptavidin (*33*) can convey more streptavidin and so more radiolabeled biotin onto the tumor. Streptavidin, however, may be more immunogenic than avidin when injected in humans (unpublished data). Methods to block this response are currently under evaluation and it is anticipated that advances in molecular biology and recombinant DNA technology will contribute significantly to circumvent this problem.

The potential advantage in cancer therapy of this pretargeting technique with respect to the use of directly labeled antibodies lies in the lower toxicity observed, allowing, in a pilot study (*34*), administration of high doses of ^{90}Y without bone marrow suppression. The improvements in terms of absolute amount of radioactivity per gram of tumor are, however, not yet satisfactory.

Increasing the dose of unlabeled antibodies, optimizing the amount of chase and administering, in the last step, high specificity activity of radioconjugated should improve the absolute quantity of radiolabel in the target.

Refinements of clinical protocols such as the use of streptavidin instead of avidin in the second step and the introduction of a second chase, under evaluation in our institutions, may play an important role in the future success of antibody-guided therapy of small ocular neoplastic lesions.

ACKNOWLEDGMENTS

We thank Francesca Chiolerio, MD, of the Società Prodotti Antibiotici, and Massimo Mariani, MD, of Sorin Biomedica, for expert preparation of the reagents used in this study, Anthony Samuel, MD for his cooperation and Fabrizio Veglia for statistical analysis. This work was supported in part by a grant from National Research Council (PF ACRO-CNR), grant 31-32586.91 (H.R. Macke) from the Swiss National Science Foundation and the Regionale Krebsliga beider Basel.

REFERENCES

1. Bomanji J, Nimmon CC, Hungerford JL, Solanki K, Granowska M, Britton KE. Ocular radioimmunoscintigraphy: sensitivity and practical considerations. *J Nucl Med* 1988; 29:1031–1044.
2. Larson SM. Biologic characterization of melanoma tumors by antigen specific targeting of radiolabeled anti-tumor antibodies. *J Nucl Med* 1991;32:287–291.
3. Buraggi GL, Callegaro L, Mariani G, et al. Imaging with ^{131}I-labeled monoclonal antibodies to a high molecular weight melanoma-associated antigen in patients with melanoma: efficacy of whole immunoglobulin and its $F(ab')_2$ fragments. *Cancer Res* 1985;45:3378–3387.
4. Bomanji J, Garner A, Prasad J, et al. Characterization of ocular melanoma with cutaneous melanoma antibodies. *Br J Ophthalmol* 1987;71:647–650.
5. Bomanji J, Hungerford JL, Granowska M, Britton KE. Radioimmunoscintigraphy of ocular melanoma with ^{99m}Tc-labeled cutaneous melanoma antibody fragments. *Br J Ophthalmol* 1987;71:651–658.
6. Scheidhauer K, Markl A, Leinsinger G, et al. Immunoscintigraphy in intraocular melanoma. *Nucl Med Commun* 1988;9:669–679.
7. Schaling DF, van der Pol JP, Jager MJ, van Kroonenburgh MJPG, Oosterhuis JA, Ruiter DJ. Radioimmunoscintigraphy and immunohistochemistry with melanoma-associated monoclonal antibodies in choroidal melanoma: a comparison of the clinical and immunohistochemical results. *Br J Ophthalmol* 1990;74:538–541.
8. Goodwin DA. Pharmacokinetics and antibodies. *J Nucl Med* 1987;28:1358–1362.
9. Messa C, Perani D, Lucignani G, et al. High-resolution technetium-99m-HMPAO SPECT in patients with probable Alzheimer's disease: comparison with fluorine-18-FDG PET. *J Nucl Med* 1994;35:210–216.
10. Paganelli G, Magnani P, Zito F, et al. Three-step monoclonal antibody tumor targeting in carcinoembryonic antigen-positive patients. *Cancer Res* 1991;51:5960–5966.
11. Lucignani G, Paganelli G, Modorati G, et al. MRI, antibody-guided scintigraphy and glucose metabolism in uveal melanoma. *J Comput Assist Tomogr* 1992;16:77–83.
12. Koch P, Maecke HR. Technetium-99m-labeled biotin conjugate in a tumor pretargeting approach with monoclonal antibodies. *Angewandte Chemie* 1992;31:1507–1509.
13. Paganelli G, Pervez S, Siccardi AG, et al. Intraperitoneal radio-localization of tumors pretargeted by biotinylated monoclonal antibodies. *Int J Cancer* 1990;45:1184–1189.
14. Hnatowich DJ, Virzi F, Rusckowski M. Investigations of avidin and biotin for imaging applications. *J Nucl Med* 1987;28:1294–1302.
15. Chang LT. A method for attenuation correction in radionuclide computed tomography. *IEEE Trans Nucl Sci* 1978;NS-25:638–643.
16. Armitage P, Berry G. *Statistical methods in medical research.* Oxford: Blackwell Scientific Publications; 1987:107–110.
17. Kessler RM, Ellis JR, Murray E. Analysis of emission tomographic scan data: limitations imposed by resolution and background. *J Comput Assist Tomogr* 1984;8: 514–522.
18. Seccamani E, Tattanelli M, Mariani M, Spranzi E, Scassellati GA, Siccardi AG. A simple qualitative determination of human antibodies to murine immunoglobulins (HAMA) in serum samples. *Nucl Med Biol* 1989;2:167–170.
19. Shields JA. Current approaches to the diagnosis and management of choroidal melanomas. *Surv Ophthalmol* 1977;21:433–463.
20. Mafee MF, Peyman GA, Peace GH, Cohen SB, Mitchell MW. Magnetic resonance imaging in the evaluation and differentiation of uveal melanoma. *Ophthalmology* 1987;94:341–348.
21. Peyster RG, Augsburger JJ, Shields A, Hershey BL, Eagle R, Haskin ME. Intraocular tumors: evaluation with MR imaging. *Radiology* 1988;168:773–779.
22. The Collaborative Ocular Melanoma Study Group. Accuracy of diagnosis of choroidal melanomas in the Collaborative Ocular Melanoma Study Group: COMS report 1. *Arch Ophthalmol* 1990;108:1268–1273.
23. Shields JA, Augsburger JJ, Brown GC, Stephens RF. The differential diagnosis of posterior uveal melanoma. *Ophthalmology* 1980;87:518–522.
24. Chang M, Zimmerman LE, McLean I. The persisting pseudomelanoma problem. *Arch Ophthalmol* 1984;102:726–727.
25. Shields JA, Shields CL. Current management of posterior uveal melanoma. *Mayo Clin Proc* 1993;68:1196–1200.
26. Paganelli G, Magnani P, Zito F, et al. Pretargeted immunodetection in glioma patients: tumor localization and single-photon emission tomography imaging of [^{99m}Tc]PnAO-biotin. *Eur J Nucl Med* 1994;21:314–321.
27. Dosio F, Magnani P, Paganelli G, Samuel A, Chiesa G, Fazio F. Three-step tumor pretargeting in lung cancer. *J Nucl Biol Med* 1994;37:228–233.
28. Bomanji J, Hungerford JL, Granowska M, Britton KE. Uptake of ^{99m}Tc-labeled $(Fab')_2$ fragments of monoclonal antibody 225.28S by a benign ocular nevus. *Eur J Nucl Med* 1988;14:165–166.
29. Scheidler J, Leinsinger G, Kirsch CM, Scheiffarth OF, Stefani FH, Riedel KG. Immunostaining of choroidal melanoma: assessment of its diagnostic accuracy and limitations in 101 cases. *Br J Ophthalmol* 1992;76:457–460.
30. Paganelli G, Magnani P, Siccardi AG, Fazio F. Applications of the avidin/biotin system for tumor targeting. In: Goldenberg D, ed. *Cancer therapy with radiolabeled antibodies.* Orlando: CRC Press; 1995:239–254.
31. Natali PG, Bigotti A, Cavaliere R, et al. Heterogeneous expression of melanoma-associated antigens and HLA antigens by primary and multiple metastatic lesions removed from patients with melanoma. *Cancer Res* 1985;45:2882–2889.
32. Matzku S, Kirchgessner H, Schmid U, Temponi M, Ferrone S. Melanoma targeting with a cocktail of monoclonal antibodies to distinct determinants of the human HMW-MAA. *J Nucl Med* 1989;30:390–397.
33. Schechter B, Silberman R, Arnon R, Wilchek M. Tissue distribution of avidin and streptavidin injected into mice: effect of avidin carbohydrate, streptavidin truncation and exogenous biotin. *Eur J Biochem* 1990;189:327–331.
34. Paganelli G, Magnani P, Meares C, et al. Antibody-guided therapy of CEA-positive tumors using biotinylated monoclonal antibodies, avidin and ^{90}Y-DOTA-biotin: initial evaluation [Abstract]. *J Nucl Med* 1993;34(suppl 5):94P.